

# Policy Supervectors: General Characterization of Agents by their Behaviour

Anssi Kanervisto, Tomi Kinnunen, Ville Hautamäki

University of Eastern Finland, School of Computing  
P-O-BOX 111, 80101 Joensuu, Finland  
anssk@uef.fi

## Abstract

By studying the underlying policies of decision-making agents, we can learn about their shortcomings and potentially improve them. Traditionally, this has been done either by examining the agent’s implementation, its behaviour while it is being executed, its performance with a reward/fitness function or by visualizing the density of states the agent visits. However, these methods fail to describe the policy’s behaviour in complex, high-dimensional environments or do not scale to thousands of policies, which is required when studying training algorithms. We propose *policy supervectors* for characterizing agents by the distribution of states they visit, adopting successful techniques from the area of speech technology. Policy supervectors can characterize policies regardless of their design philosophy (*e.g.* rule-based vs. neural networks) and scale to thousands of policies on a single workstation machine. We demonstrate method’s applicability by studying the evolution of policies during reinforcement learning, evolutionary training and imitation learning, providing insight on *e.g.* how the search space of evolutionary algorithms is also reflected in agent’s behaviour, not just in the parameters.

## Introduction

An *agent* (Sutton and Barto 2018) is a decision-making creature that acts in an environment by observing it and taking actions according to its *policy*, such as automated chess players or self-driving cars (Bojarski et al. 2016). The simplest policies work on simple rules such as “always accelerate” or “turn right” or with a combination of them. *Reinforcement learning* (RL) (Sutton and Barto 2018) provides a mathematical framework to *train* policies by trying out different actions and using the provided reward to learn what actions are desired. *Genetic algorithms* (GA) (Mitchell 1998) and *evolution strategies* (ES) (Hansen and Ostermeier 2001) take inspiration from biology and evolve a population of different policies, keeping only the promising ones for the next generation, mutating and combining them via crossover to test out different policies.

To improve these training algorithms, the *de facto* tool is to measure how well they perform in the task and see which changes to the algorithm improve the result (Jordan et al. 2020; Henderson et al. 2017). While this clearly tells if policy is doing well in the task, reward is only a one-dimensional characterization of the policy’s behaviour. Say,

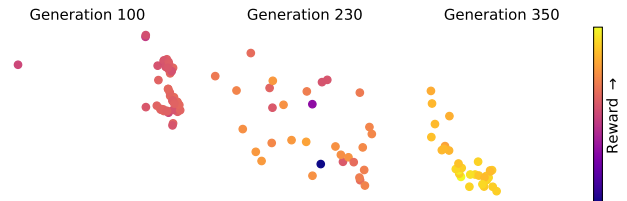


Figure 1: Evolution of policies under covariance matrix adaptation evolution strategies (CMA-ES) (Hansen and Ostermeier 2001) where each point represents policy by their *behaviour* (policy supervector) rather than their parameters, after dimensionality reduction with t-SNE. The characteristic behaviour of CMA-ES where the search space enlarges and then tightens is also visible in the policies’ behaviour.

we have two different robots both solve a maze but only one of them pressed the button in the end required to receive reward. Clearly the two policies are practically the same but the reward signal tells an opposite story. A manual inspection of robot’s behaviour would reveal this, but such method does not scale up to many different robots, *e.g.* if we want to study how training algorithms evolve policies. We could compare the underlying implementation of the two robots but is not possible if the two robots have two different design principles, like a neural network vs. a rule-based system.

Instead we propose focusing on the states the policy visits. Intuitively, policies are different if they visit different states in the environment. Such approach has already been used, *e.g.* by plotting a heatmap of visited x/y-coordinates (Pitis et al. 2020) or using or by using dimensionality-reduction to visualize what policy does (Hernandez et al. 2020), with such analysis being helpful in improving exploration of RL agents (Bellemare et al. 2016; Pathak et al. 2017). However, this kind of visualization is limited to specific environments where we have such descriptive, low-dimensional vectors such as x-y coordinates or rely on dimensional reduction to produce 2D points from higher-dimensional vectors. Even then, time and space complexity of methods like t-SNE (Maaten and Hinton 2008) grow quadratically with the number of data points (Maaten and Hinton 2008).

We propose a method that generalizes the analysis of visited states for any policy and environment by building a dis-

tribution of visited states, and then compare policies by the parameters of this distribution. This *policy supervector* borrows successful techniques used in the speech technology field, where *speaker supervectors* are used to model speakers and identify them from each other (Kinnunen and Li 2010). With this method we can compare thousands of policies from different training algorithms and visualize their evolution, with an example in Figure 1. We also study the effect of method’s hyperparameters as well as demonstrate its applicability by studying the evolution of policies under RL and imitation learning training.

## Related work

**Comparing policies.** The *de facto* method for comparing policies is by evaluating their performance in a task (Jordan et al. 2020). Moving outside rewards, related work has compared policies of different algorithms by plotting the density of visited states on a x/y plane (Pitis et al. 2020; Conti et al. 2018). Hernandez et al. (2020) make use of dimensional reduction to plot fixed-length trajectories of different self-play algorithms to study evolution of policies, while Wang et al. (2017) train a recurrent encoder to transform varying-length trajectories into a fixed vector. Trust-region policy optimization (Schulman et al. 2015) measures KL-divergence of action distributions between updated and previous policy and constrains this distance. Policies can also be defined by compact descriptions such as a genome defining a network and its weights (Gaier and Ha 2019a) or providing seeds for a pseudo-random generator that generates desired network parameters (Such et al. 2017).

**Distribution of visited states as part of learning algorithm.** Keeping track of which states agent has visited can be used to encourage exploring different states (Bellemare et al. 2016), with other methods proposing to use *e.g.* prediction error as a measure of how often state has been seen (Burda et al. 2018). Using visited states as a measure of “novelty”, Eysenbach et al. (2018) create a set of diverse policies where each policy visits different states, and Conti et al. (2018) combine the metric with evolutionary algorithms to encourage testing novel policies. Imitation learning has also been framed as a task of matching demonstrator’s state-action distribution with success (Ho and Ermon 2016), and terms related to distribution of visited states or trajectories are a common tool in offline reinforcement learning where goal is to learn from a fixed set of data (Levine et al. 2020).

## Preliminaries

We will model the environments akin to *partially observable Markov decision process* (POMDP) (Sutton and Barto 2018), where the agent may observe only part of the full state  $s \in \mathcal{S}$ . The environment begins in an initial state  $s_0 \sim p(s_0)$ . An *observation*  $o \in \mathcal{O}$  is an unknown and stochastic function of the state  $o \sim p(o|s)$ . After receiving an observation the *policy* (agent)  $\pi \in \Pi$  provides an *action*  $a \in \mathcal{A}$ , either as a deterministic function  $a = \pi(o)$  or as a stochastic function  $a \sim \pi(o)$ . With the given action the state of the environment is then evolved based on

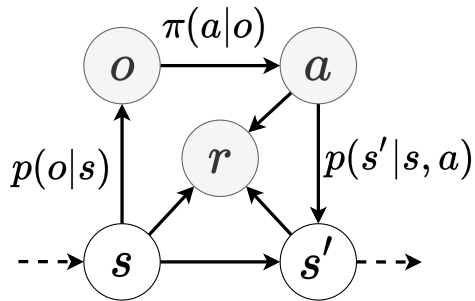


Figure 2: The data generation process of a single step of running policy  $\pi$  on a POMDP. Shaded nodes represent observable variables, with associated distributions noted next to arrows. Rewards  $r$  distribution is  $p(r|s, a, s')$ .

a stochastic function  $s' \sim p(s'|s, a)$  (*transition dynamics*), and agent is provided with a reward  $r \sim p(r|s, a, s')$ . This process repeats until environments lands into a terminal state  $s_T \in \mathcal{T}$ ,  $\mathcal{T} \subset \mathcal{S}$ . An *episode* is a full game from an initial state to the terminal state, where *trajectory* refers to the tuple of experienced states, actions and rewards in the process. An environment is defined by tuple  $(\mathcal{S}, \mathcal{A}, p(s_0), p(o|s), p(s'|s, a), p(r|s, a, s'), \mathcal{T})$ .

To model probability density  $p(\mathbf{x})$  of a random variable  $\mathbf{x} \in \mathbb{R}^d$ , we will make use of *Gaussian mixture models* (GMM) (McLachlan and Basford 1988). GMMs consist of  $K$  Gaussian distributions, each with their own weights  $w_i \in [0, 1]$ ,  $\sum_i w_i = 1$ ,  $i \in \{1 \dots K\}$ , means  $\mu_i \in \mathbb{R}^d$  and covariance matrices  $\Sigma_i \in \mathbb{R}^{d \times d}$ . The probability density function of a GMM is then defined as  $p(\mathbf{x}) = \sum_{i=1}^K w_i p_i(\mathbf{x})$ , where  $p_i(\mathbf{x})$  is likelihood function of multivariate Gaussian distribution  $\mathcal{N}(\mu_i, \Sigma_i)$ . There is no closed-form solution for maximizing the likelihood of parameters given some data, but with some initial parameters *Expectation-Maximization* (EM) algorithm (Dempster, Laird, and Rubin 1977) provides a local maximum likelihood-estimate of the parameters.

## Comparing policies

Consider a *fixed* environment as described above and two or more policies for it. To facilitate a meaningful comparison of policies, we need to define what we mean by “different” policies. Informally we say two policies are different if their behaviour is different. If both policies use the same design philosophy, we could compare their parameters and implementation, like neural networks or rules. If these parameters differ, we could say the two policies are different. However, this limits comparison to policies to only those with similar underlying implementation, and even then the comparison might be difficult. A rule-based system may have too many levels of logic, and a neural network may output the same values even with different sets of weights, like when the activation function clip unit activations.

Instead let us study what kind of data we have available by running the policies on an environment. Figure 2 shows the data generation process and the variables that are available to us. The most commonly used variable of these is the re-

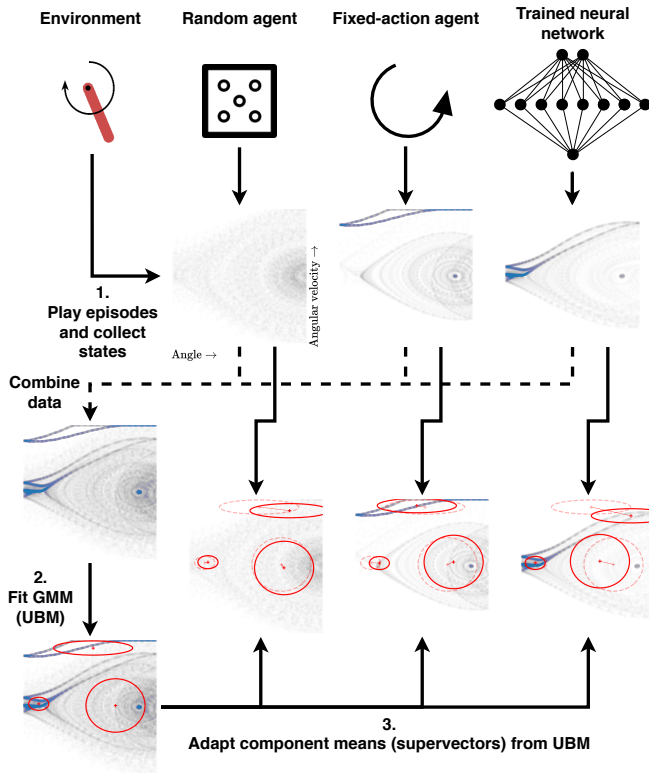


Figure 3: Demonstration of the proposed method computing policy supervectors for three policies in the Pendulum environment, using real data and policies. Each faint dot represents a single state of Pendulum environment (angle and angular velocity of the pendulum), and red circles represent Gaussian components of the GMMs.

ward: the average episodic reward is a the *de facto* metric for comparing policies by comparing their performance, either the average reward or distribution of rewards (Jordan et al. 2020). In fact, in RL the optimal policy is defined as one that reaches maximum possible reward starting from any state (Sutton and Barto 2018). If two policies have different distribution for rewards, then they are different, as policy is the only thing that can change the generation process. However different policies can be optimal and still share the same the same value function, *i.e.* the same expected sum of rewards in any state (Sutton and Barto 2018).

Another option is to compare the actions the two policies take or measure the KL-divergence of the action distributions, under the same observations. However, similar to the commentary in Eysenbach et al. (2018), we argue that this may capture non-existent differences between policies. As an extreme example, let the environment transition dynamics  $p(s'|s, a)$  be independent of action, *i.e.*  $p(s'|s, a) = p(s'|s)$ ,  $\forall a \in \mathcal{A}$ . If we compare actions of the two policies, which might be different, we end up with some measure of difference between policies. But in reality, they both had the same, zero effect on the environment, and to an outside observer both agents appear the same. Practical examples in-

clude a video game player trying to execute an invalid action or a robot trying to turn a joint beyond allowed limits.

As already proposed and used by others (such as Pitis et al.; Bellemare et al.), our approach is to compare policies by the states they visit. Informally, we say that the two policies are different if they visit different states such as different locations. Formally, we define the distribution of the states policy visits as  $p_\pi(s)$  (*state distribution*). We could then measure differences of the compared policies through their KL-divergence or Wasserstein-metric between their state distributions, with no restrictions on how the policy should be implemented. The only assumption we need is that the environment remains fixed, in which case the policy itself is the only thing that can change what states are visited. Alas, the full state information may not be obtainable even by an outside observer in a partially observable environment. However, since the observation-distribution  $p(o|s)$  is fixed, observations will also remain fixed for all policies and we can model its distribution instead. In fact, we can combine information from actions, per-step rewards and observations and model the joint-distribution  $p_\pi(o, a, r)$ , or come up with a new function  $f(s)$  that transforms the current environment state, or a part of it, into vector that is believed to describe the policies (*e.g.* x-y coordinates). We will continue the notion  $p_\pi(s)$  and term “state distribution”, but it can be interchanged with any of the previous suggestions.

Alas, a closed-form and computable solution for  $p_\pi(s)$  rarely exists since the underlying environment dynamics are unknown. We have to resort to sampling by running the policy on the environment for multiple different initial states, and then fit our favorite density estimator on it. Unfortunately, given the complexity of some of the environments (*e.g.* Atari games (Bellemare et al. 2013)), we may need to gather millions of states per policy for a trustworthy density estimation. This renders kernel-based density estimators unusable, given their poor scaling with an increasing number of data. Simple parametric distributions like Gaussian-distribution are computationally light and have closed-form solutions for estimating the parameters, but likely fail to properly model the multi-modal nature of the data. For an example, see Figure 3 where even in a simple, 2D environment a single policy can have distinct clusters in the distribution of visited states (fixed-action agent).

### Supervectors for describing policies

If a single Gaussian is not enough to model the distribution, what about a mixture of them? GMMs can be used to model multi-modal data, and with enough components they can model almost any continuous distribution to an arbitrary accuracy (Bishop 2006). However, measuring the difference between two GMMs using KL-divergence requires sampling data points from one distribution and testing likelihood on another. We found this combination of fitting one GMM per policy and estimating KL-divergences via sampling to be computationally prohibitively expensive when *e.g.* trying to study evolution of a policy of a RL algorithm with hundreds of saved versions.

Instead we draw inspiration from the field of speech processing. In specific, we adopt GMM-based methods from

---

**Algorithm 1:** Extracting policy supervectors. Python-like pseudo-code with OpenAI Gym environments.

---

**Input:** An environment  $env$ , a set of policies we wish to study  $\pi_n, n \in \{1 \dots N\}$ , number of GMM components  $K$  and number of states to gather per policy  $T$ .

```
#Gather shared and individual
  datasets of states per policy.
```

```
 $D_n = [], n \in \{1 \dots N\}$ 
```

```
 $D_{ubm} = []$ 
```

```
for  $n \in \{1 \dots N\}$  do
```

```
   $s = env.reset()$ 
```

```
  for  $t \in \{1 \dots T\}$  do
```

```
     $D_n.append(s)$ 
```

```
     $D_{ubm.append}(s)$ 
```

```
     $a = \pi_n(s)$ 
```

```
     $s = env.step(a)$ 
```

```
  end
```

```
end
```

```
#Fit a GMM with  $K$  components (UBM).
```

```
 $(\mu_{ubm}, \Sigma_{ubm}, w_{ubm}) = gmm.fit(D_{ubm}, K)$ 
```

```
#Extract supervectors.
```

```
for  $n \in \{1 \dots N\}$  do
```

```
  pivector $_n = []$ 
```

```
  for  $i \in \{1 \dots K\}$  do
```

```
    #MAP-adapt  $i^{\text{th}}$  mean as in
    (1)–(5).
```

```
     $\hat{\mu}_i = \text{mapAdapt}(\mu_{ubm}, \Sigma_{ubm}, w_{ubm}, D_n)$ 
```

```
    #Concatenate mean to the
    supervector.
```

```
    supervector $_n =$ 
```

```
    concatenate(supervector $_n, \hat{\mu}_i)$ 
```

```
  end
```

```
end
```

**Output:** UBM parameters  $(\mu_{ubm}, \Sigma_{ubm}, w_{ubm})$  and policy supervectors  $\text{supervector}_n, n \in \{1 \dots N\}$

---

the domain of automatic speaker verification where GMMs are used to model speaker features within individual audio recordings with success (Kinnunen and Li 2010). The same problem of fitting large GMMs on large amount of data exists in speech processing, too, until Reynolds, Quatieri, and Dunn (2000) suggested using an *universal background model* (UBM) to model distribution of the features independent of the speaker. A GMM is trained on a large pool of speaker features from different speakers to form a GMM-UBM. This was then used in two ways: a speaker-specific GMM is adapted from the GMM-UBM parameters with *Maximum a Posteriori* (MAP) adaptation, and speaker is then verified by measuring if given features are closer to speaker-specific GMM or the GMM-UBM. If latter, the speaker is more likely is not the claimed speaker. Alternatively, one can concatenate the adapted GMM’s parameters into a long vector, called a *supervector* (Campbell, Sturim,

and Reynolds 2006), describing the speaker with a fixed-length vector which can be used in classification and verification (Kinnunen and Li 2010). Despite intentionally forgetting that speech is a time-dependent process, the assumption of identical and independently distributed data (iid.) is used here and it has been found useful in speaker verification (Reynolds, Quatieri, and Dunn 2000).

We propose to do the same for policies by training a large GMM-UBM (later just “UBM”) on a pool of data from all policies of interest and adapting per-policy GMMs from the UBM. Figure 3 demonstrates this process visually, and Algorithm 1 includes a pseudo-code of this process. For all of the policies we wish to study, we run it on the environment for a desired amount of episodes, store the states (or observations and/or actions), use this data from all of the policies to train the UBM and then adapt a per-policy GMM with the policy’s data. Under Bayesian view, the UBM represents an informative prior while the adapted GMM is a point estimate of the posterior, but we also include the same data used to derive posterior in the prior. We treat the UBM as a common feature-extractor for all policies, ensuring all the adapted GMMs are identifiable and comparable to each other, *i.e.* components can be compared index-wise (Bishop 2006). By including data from all policies ensures the prior covers all states visited by the policies. Using data in Figure 3 as an example, if we did not include data from “fixed-action agent” in UBM training, it would not cover the up-most data and the learned priori would be misleading (it does not represent all data that can be generated). We call the adapted parameters a *policy supervector*.

Formally, consider  $N$  policies  $\pi_i, i \in \{1 \dots N\}$  that we want to study. For each policy we play  $M$  episodes in the environment, record the  $d$ -dimensional states  $s \in \mathbb{R}^d$  experienced during the episodes and store them to a per-policy dataset  $D_i = (s_1, s_2, \dots)$ . All of this data is pooled together into an UBM-training set  $D_{ubm} = (D_1, \dots, D_N)$ . This set is then used to fit an UBM with  $K$  components and parameters  $\mu_{ubm} \in \mathbb{R}^{K \times d}, \Sigma_{ubm} \in \mathbb{R}^{K \times d \times d}$  and  $w_{ubm} \in \mathbb{R}^K, w_i \geq 0, \sum_i w_i = 1$  with EM-algorithm until convergence. We can then perform MAP-adaptation on a per-policy dataset  $D = (s_1 \dots s_T)$  to obtain adapted mean  $\hat{\mu}_i$  of  $i^{\text{th}}$  component with (Reynolds, Quatieri, and Dunn 2000)

$$p(i|s_t) = \frac{w_i \mathcal{N}(\mu_i, \Sigma_i)}{\sum_{k=1}^K w_k \mathcal{N}(\mu_k, \Sigma_k)} \quad (1)$$

$$n_i = \sum_{t=1}^T p(i|s_t) \quad (2)$$

$$E_i(D) = \frac{\sum_{t=1}^T p(i|s_t) s_t}{n_i} \quad (3)$$

$$\alpha_i = \frac{n_i}{n_i + r} \quad (4)$$

$$\hat{\mu}_i = \alpha_i E_i(D) + (1 - \alpha_i) \mu_i, \quad (5)$$

where  $r$  is a *relevance factor* used to weight how much new data can affect the adapted mean. The adapted means can be used as-is to describe the policy with variable-length trajectories as a fixed-length vector. Alternatively, Campbell,

Sturim, and Reynolds (2006) show that an upper-bound for KL-divergence of means of two adapted GMMs  $\mu_a$  and  $\mu_b$  is

$$d_{\text{KL}}(\mu_a, \mu_b) \geq \frac{1}{2} \sum_{i=1}^K w_{\text{ubm}}^i (\mu_a^i - \mu_b^i) \Sigma_{\text{ubm}}^{-1} (\mu_a^i - \mu_b^i). \quad (6)$$

Unlike KL-divergence, this upper-bound is a proper distance metric (Campbell, Sturim, and Reynolds 2006). We only adapt means in this work following speaker verification (Kinnunen and Li 2010) and also to allow use of the distance metric, but covariances and weights can be adapted in similar fashion (see Reynolds, Quatieri, and Dunn (2000) equations (11)-(13)).

**Advantages.** Thanks to requiring only lengthy training of a GMM, this procedure scales up to thousands of different policies on a single workstation-level machine, which we demonstrate below. This method is not limited to specific type of state vectors modelling the distributions (*e.g.* observations directly or latent vectors of an image (Chen 2020)), and similarly this method is not limited to specific types of policy design principles. This method also does not require further assumptions on the set of policies that are being analyzed, *e.g.* we do not need to know if some of the policies are different. Finally, the core algorithm is simple, with the majority of the complexity contained in the MAP-adaptation and distance between adapted GMMs (Equations (1)-(6)). Implementations for fitting a GMM with EM-algorithm exist in various libraries like scikit-learn (Pedregosa et al. 2011).

**Limitations.** While theoretically any type of state vector can be used, computing resources become a restriction quickly. As dimensionality of state vectors increase, more data is required for a reliable density estimation (curse of dimensionality) as well more computer memory is required for the EM-algorithm. This also makes collecting data slower, especially if the environment is slow. Compare this to measuring KL-divergence of actions where a single, fixed dataset can be used. There is no one answer on what data should be used for state vectors, as each variable may or may not help separating different policies, depending on the environment. The most certain solution is to include as much information as possible, but this quickly runs to the practical issues discussed above. Finally, while the assumption of a fixed environment is practical in case of simulations, it may be difficult to extend it to robotics and real world where actuators and sensors can change over time due to different surrounding conditions like temperature.

## Experiments and results

We demonstrate use cases for the proposed method by running experiments related to previously reported results and insights, but under this new view of comparing what states are visited. We will also study the effect of the hyperparameters, namely the number of Gaussian components for the UBM and amount of data gathered per policy. We use five classic-control environments from the OpenAI Gym library (Brockman et al. 2016) which include low dimensional environments (Cartpole, Pendulum and Acrobot) as well as

two more complex environments (Lunarlander and Bipedal-walker). Details on experimental setup are available in Appendix along with the source code in the supplementary material. Results shown here are representative examples with all results included in Appendix. Code for experiments is available at <https://github.com/Miffyli/policy-supervectors>.

### Effect of hyperparameters

As collecting the states the policy visits is one of the bottlenecks, this raises the question “how much data do we need to collect to obtain reliable results?”. At the same time we also have to select the number of Gaussian components used in the GMM. Theoretically, more is better as seen in speaker verification (Kinnunen and Li 2010; Kinnunen et al. 2009), but this may be practically prohibitive (high memory usage). Both of these are also tied to the dimensionality of the state vectors, with higher-dimensional vectors requiring more data for representative examples. To study this we take a fixed set of policies and measure distance between them (distance matrix) under different settings. Policies are obtained by training *proximal policy optimization* (PPO) (Schulman et al. 2017) agents and saving one hundred versions of the policy during training.

To measure variance in results we use *coefficient of variation* (CV) (Everitt and Skrondal 2002)  $\sigma/\mu$  over the different repetitions of the same experiment, starting from a fixed policy. CV tells us how much the resulting distance differs between runs but does not describe how far off it is from the “true” value: since policies are fixed, the distance between them should be fixed, which we could obtain with infinite amount of data and a large GMM. To study this error we estimate it with hundred trajectories of data, and then measure relative error to this result under different amounts of data and components, including other repetitions with hundred trajectories of data.

Above metrics provide insight in how results change between repetitions but not in how well supervectors separate between different policies. To analyze this we compare the average distance between all policies to the average distance between different policies (ratio), where policies are different if they reach different average rewards in the environment. If two policies have a substantially different reward they must behave differently in some way, but as argued above, this does not tell the extent of the difference. We will report the average distance divided by the average distance of different policies to share “lower is better” mentality with the error metrics above.

Figure 5 shows the results with remaining per-environments plots in the Appendix. The error and variance of distance matrices is consistent across environments, where the change in results between results decreases with more data per policy combined with more components. The distance ratio is less than one (*i.e.* different policies are further apart than policies on average) unless too many components are used with too little data. In most cases the ratio stays the same over different amounts of components, with an exception in LunarLander where the ratio doubles as we move from one/two components to 64 components. This demonstrates that the correct amount of components

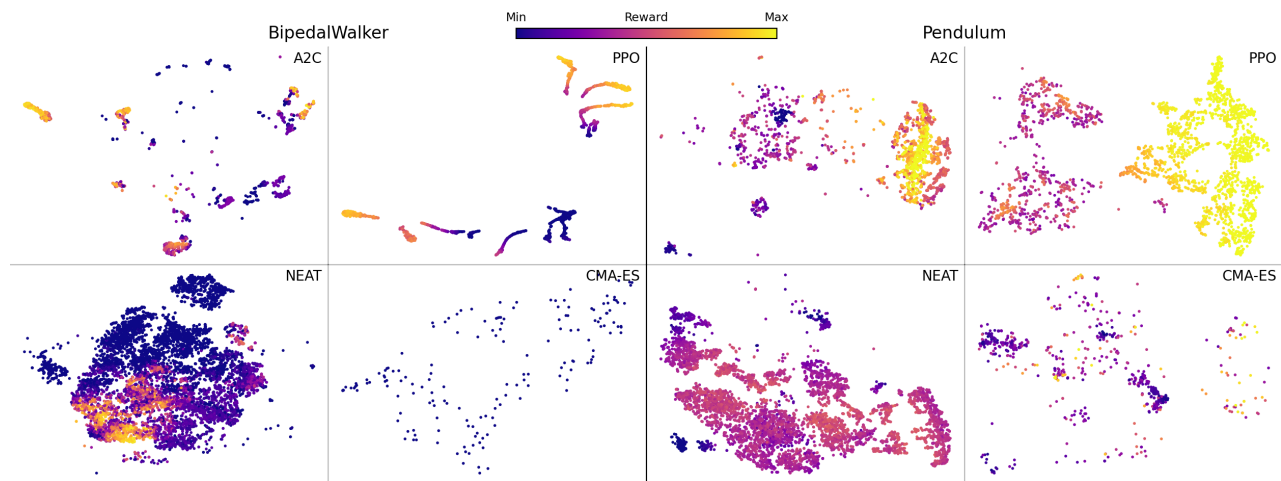


Figure 4: t-SNE plot of evolution of policies under different training algorithms. Plots under same environment share the same plot scales. Rewards are scaled according to minimal and maximal obtainable reward per environment.

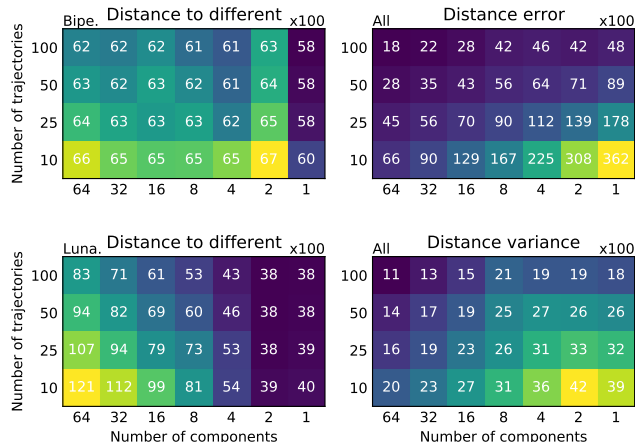


Figure 5: Lower is better. Effect of hyperparameters on distance metric between different policies (left, two environments), error in distance matrix (upper-right, over all environments) and variance of distance matrix ( $\sigma/\mu$ , lower-right). All results are averaged over three repetitions.

is dependent on the environment, but generally more will translate to stabler results between repetitions. Increasing the amount of data improved the performance in all metrics. All in all, we suggest to use as much data as possible with 100 trajectories per policy being a good starting point along with 64 components for the UBM.

### Overview of different training algorithms

One of the questions that originally sparked this work was “how does training of evolutionary methods compare to reinforcement learning?” Evolution-based methods like *neuroevolution of augmenting topologies* (NEAT) (Stanley and Miikkulainen 2002) and CMA-ES explore by modifying promising solutions and testing which location of the parameter space works better (Hansen and Ostermeier 2001),

while on-policy RL methods like *advantage actor critic* (A2C) (Mnih et al. 2016) and PPO update a single policy towards higher episodic reward. For a visual overview of these training algorithms we train them on the environments and store evolution candidates and policy versions at different points of training, extract their policy supervectors and plot the resulting points with t-SNE (Maaten and Hinton 2008). The distance for t-SNE is computed using (6). Hypothesis is that evolution-based methods cover a wider area of policies, while RL algorithms remain in a small region.

Figure 4 shows resulting t-SNE plots for two environments with five A2C and PPO runs as well as one NEAT and CMA-ES run (rest of the plots are in the Appendix). In total we compare ten to thirty thousand policies per environment and rely on sub-sampling the whole dataset to fit the UBM fitting on the machine’s memory (64GB). Different amounts of points per algorithm is a result of different training hyperparameters. Evolutionary algorithms include policies from a wide area whereas RL algorithms form smaller clouds. While studying the evolution of CMA-ES we noted the behaviour of tested policies follows the training procedure, where the search space enlarges towards the direction of better performance and then tightens, highlighted in Figure 1. Finally, when comparing A2C and PPO policies, A2C has larger-variance clouds of policies while PPO training runs form “snakes” in more complicated environments. We can also see the benefit of the proposed method over comparing policies by their performance: many policies share the same average reward but are distant points in these plots.

### Effect of trust-region constraints on policy gradient algorithms

Schulman et al. (2015) show that by restricting the amount policy is changed per update is guaranteed to improve the policy, and PPO provides a simpler algorithm to achieve this. However, recent results have raised doubts on the performance gains of the core PPO algorithm (ratio-clip value  $\epsilon$ ) and demonstrate how in practice this trust region is con-

$\epsilon$	Cart	Lunar	Bipedal	Corr( $R, d$ )
.01	2.0±0.1	4.5±0.5	23.6±1.1	-0.02±0.33
.1	7.7±1.6	9.9±0.5	10.7±1.5	-0.34±0.14
.5	15.3±1.7	15.0±0.7	12.0±2.6	-0.29±0.22
1.0	14.0±4.0	18.9±2.5	25.1±10.9	-0.17±0.29
5.0	20.2±2.6	22.9±4.3	25.4±7.2	-0.21±0.29
10.0	14.9±4.9	21.5±2.6	51.5±21.1	-0.14±0.30
A2C	6.5±0.7	29.4±4.3	61.8±16.6	0.00±0.30

Table 1: Total distance traveled by policy during PPO training with different ratio-clipping values  $\epsilon$ , averaged over five training runs along with standard deviation. Corr( $R, d$ ) is Pearson correlation between average episodic reward and distance to next policy in training. Rest of the results are available in the Appendix.

stantly violated while studying KL-divergence between policies’ actions (Engstrom et al. 2020). In the above visual overview we noted how PPO policies are clumped closer together than A2C policies, indicating that this restriction applies to behaviour of the policies as well. We hypothesise this is so, as a small change in actions should only lead to a small change in states visited, but the KL-divergence of action distributions does not capture the true effect on the environment, as argued above.

To study this, we train PPO agents with different ratio-clip values  $\epsilon$ , where lower value should restrict updates to smaller changes in the policy. We also include experiments with A2C which do not restrict policy changes. We measure total distance traveled by the policy by saving 50 versions of the policy during training, computing distance between successive policies’ and summing them together to measure total distance traveled, including any oscillation back-and-forth.

Results in Table 1 show how indeed lower ratio-clip value leads to policy traveling a shorter distance in total. In higher-dimensional environments A2C also travels notable longer distances than PPO. These results concur with the theory behind PPO’s ratio-clipping and show it limits the changes to policy’s behaviour as well.

However there are odd results, *e.g.*  $\epsilon = 0.01$  with BipedalWalker and A2C results with Cartpole. To explain these we studied the learning curves (in Appendix) and noticed a common trend: as policy got better in the task the distance traveled between saved policies decreased. Indeed, if we compute Pearson correlation between average episodic return and distance to next checkpoint (Table 1, fifth column), we see how PPO with  $\epsilon \in [0.1, 10.0]$  the correlation is negative, suggesting that there is a connection between two. With the low clipping value  $\epsilon = 0.01$  the agent struggles to improve in the task and successive-policy-distance stays constant. These results concur with observations of Engstrom et al. (2020), where the KL-distance between successive policies first increases and then decreases as training moves on.

## Policy evolution during behavioural cloning

Using a set of expert demonstrations, *behavioural cloning* (BC) (Pomerleau 1989) trains the policy as a supervised-learning task where policy predicts what action expert would have taken, given a dataset of expert’s trajectories. This can theoretically recover the original policy that generated the data, but in general BC has been proven to have poor performance guarantees (Ross, Gordon, and Bagnell 2011). Knowing that BC could recover the original policy, we test that proposed method reflects this: the policy being trained by BC approaches the expert policy. To do this we use LunarLander and BipedalWalkerHardcore environments, train PPO agents on them, collect ten trajectories of the final agent and then use BC to train a policy with these trajectories. We selected more complex environments in an attempt to bring out possible failure cases of BC. Hypothesis is that the BC policy gets closer to the expert policy during training.

Learning curve and change distance is available in the Appendix. The distance to expert policy decreases during training and there is a connection between how policy’s reward and distance to expert changes (average Pearson correlation of  $-0.465$  with standard deviation of  $0.297$ , averaged over both environments and their five repetitions), supporting the hypothesis.

## Discussion and conclusion

As we demonstrated, policy supervectors are a general way for comparing different types of policies, scales to thousands of policies, it successfully separates different policies from each other and provides a distance metric that reflects how different policies’ behaviour is. Compared to rewards alone it provides a more informative description as seen during the experiments, and it does not capture non-existent behaviour like methods studying differences in actions alone. It also does not require pre-training or additional assumptions from the policies, as long as the environment stays fixed. However this comes at the cost of requiring a large number of samples from the environment and informative description of the state, which can be difficult to obtain with slow simulators or even real world robotics.

The experiments we included, apart from the study of effects of hyperparameters, were mainly to demonstrate the applicability of the proposed method as such an analysis tool. Remaining questions for future works include, for example, studying the effect of different types of exploration methods and curiosity rewards used in the reinforcement learning (Pathak et al. 2017) or studying how different offline imitation-learning methods evolve their policies (Levine et al. 2020). This type of analysis is not just limited to studying the distances between policies, but we could also study the components (clusters) learned by the GMM. These could represent “super-states” (a group of different states), and this information can be used to see when/how policy moves from one super-state to another. With generality of the method but so many questions remaining, we believe this type of analysis will solidify existing knowledge and lead to new insights down the line.

## References

- Bellemare, M.; Srinivasan, S.; Ostrovski, G.; Schaul, T.; Saxton, D.; and Munos, R. 2016. Unifying count-based exploration and intrinsic motivation. In *Advances in neural information processing systems*, 1471–1479.
- Bellemare, M. G.; Naddaf, Y.; Veness, J.; and Bowling, M. 2013. The arcade learning environment: An evaluation platform for general agents. *Journal of Artificial Intelligence Research* 47: 253–279.
- Bishop, C. M. 2006. *Pattern recognition and machine learning*. Springer.
- Bojarski, M.; Del Testa, D.; Dworakowski, D.; Firner, B.; Flepp, B.; Goyal, P.; Jackel, L. D.; Monfort, M.; Muller, U.; Zhang, J.; et al. 2016. End to end learning for self-driving cars. *arXiv preprint arXiv:1604.07316* .
- Brockman, G.; Cheung, V.; Pettersson, L.; Schneider, J.; Schulman, J.; Tang, J.; and Zaremba, W. 2016. OpenAI Gym.
- Burda, Y.; Edwards, H.; Storkey, A.; and Klimov, O. 2018. Exploration by random network distillation. *arXiv preprint arXiv:1810.12894* .
- Campbell, W. M.; Sturim, D. E.; and Reynolds, D. A. 2006. Support vector machines using GMM supervectors for speaker verification. *IEEE signal processing letters* 13(5): 308–311.
- Chen, J. Z. 2020. Reinforcement Learning Generalization with Surprise Minimization. *arXiv preprint arXiv:2004.12399* .
- Conti, E.; Madhavan, V.; Such, F. P.; Lehman, J.; Stanley, K.; and Clune, J. 2018. Improving exploration in evolution strategies for deep reinforcement learning via a population of novelty-seeking agents. In *Advances in neural information processing systems*, 5027–5038.
- Dempster, A. P.; Laird, N. M.; and Rubin, D. B. 1977. Maximum likelihood from incomplete data via the EM algorithm. *Journal of the Royal Statistical Society: Series B (Methodological)* 39(1): 1–22.
- Engstrom, L.; Ilyas, A.; Santurkar, S.; Tsipras, D.; Janoos, F.; Rudolph, L.; and Madry, A. 2020. Implementation Matters in Deep Policy Gradients: A Case Study on PPO and TRPO. *arXiv preprint arXiv:2005.12729* .
- Everitt, B.; and Skrondal, A. 2002. *The Cambridge dictionary of statistics*, volume 106. Cambridge University Press Cambridge.
- Eysenbach, B.; Gupta, A.; Ibarz, J.; and Levine, S. 2018. Diversity is all you need: Learning skills without a reward function. *arXiv:1802.06070* .
- Gaier, A.; and Ha, D. 2019a. Weight agnostic neural networks. In *Advances in Neural Information Processing Systems*, 5364–5378.
- Gaier, A.; and Ha, D. 2019b. Weight Agnostic Neural Networks URL <https://weightagnostic.github.io>. <https://weightagnostic.github.io>.
- Hansen, N.; Akimoto, Y.; and Baudis, P. 2019. CMA-ES/pycma on Github. Zenodo, DOI:10.5281/zenodo.2559634. doi:10.5281/zenodo.2559634. URL <https://doi.org/10.5281/zenodo.2559634>.
- Hansen, N.; and Ostermeier, A. 2001. Completely derandomized self-adaptation in evolution strategies. *Evolutionary computation* 9(2): 159–195.
- Henderson, P.; Islam, R.; Bachman, P.; Pineau, J.; Precup, D.; and Meger, D. 2017. Deep reinforcement learning that matters. *arXiv preprint arXiv:1709.06560* .
- Hernandez, D.; Denamganai, K.; Devlin, S.; Samothrakis, S.; and Walker, J. A. 2020. A Comparison of Self-Play Algorithms Under a Generalized Framework. *arXiv preprint arXiv:2006.04471* .
- Hill, A.; Raffin, A.; Ernestus, M.; Gleave, A.; Kanervisto, A.; Traore, R.; Dhariwal, P.; Hesse, C.; Klimov, O.; Nichol, A.; Plappert, M.; Radford, A.; Schulman, J.; Sidor, S.; and Wu, Y. 2018. Stable Baselines. <https://github.com/hill-a/stable-baselines>.
- Ho, J.; and Ermon, S. 2016. Generative adversarial imitation learning. In *Advances in neural information processing systems*, 4565–4573.
- Jordan, S. M.; Chandak, Y.; Cohen, D.; Zhang, M.; and Thomas, P. S. 2020. Evaluating the Performance of Reinforcement Learning Algorithms. *arXiv preprint arXiv:2006.16958* .
- Kinnunen, T.; and Li, H. 2010. An overview of text-independent speaker recognition: From features to supervectors. *Speech communication* .
- Kinnunen, T.; Saastamoinen, J.; Hautamäki, V.; Vinni, M.; and Fränti, P. 2009. Comparative evaluation of maximum a posteriori vector quantization and Gaussian mixture models in speaker verification. *Pattern Recognition Letters* 30(4): 341–347.
- Levine, S.; Kumar, A.; Tucker, G.; and Fu, J. 2020. Offline reinforcement learning: Tutorial, review, and perspectives on open problems. *arXiv preprint arXiv:2005.01643* .
- Maaten, L. v. d.; and Hinton, G. 2008. Visualizing data using t-SNE. *Journal of machine learning research* 9(Nov): 2579–2605.
- McLachlan, G. J.; and Basford, K. E. 1988. Mixture models. Inference and applications to clustering. *mmia* .
- Mitchell, M. 1998. *An introduction to genetic algorithms*. MIT press.
- Mnih, V.; Badia, A. P.; Mirza, M.; Graves, A.; Lillicrap, T.; Harley, T.; Silver, D.; and Kavukcuoglu, K. 2016. Asynchronous methods for deep reinforcement learning. In *ICML*.
- Pathak, D.; Agrawal, P.; Efros, A. A.; and Darrell, T. 2017. Curiosity-driven Exploration by Self-supervised Prediction. In *ICML*.
- Pedregosa, F.; Varoquaux, G.; Gramfort, A.; Michel, V.; Thirion, B.; Grisel, O.; Blondel, M.; Prettenhofer, P.; Weiss, R.; Dubourg, V.; Vanderplas, J.; Passos, A.; Cournapeau, D.;



- Brucher, M.; Perrot, M.; and Duchesnay, E. 2011. Scikit-learn: Machine Learning in Python. *Journal of Machine Learning Research* 12: 2825–2830.
- Pitis, S.; Chan, H.; Zhao, S.; Stadie, B.; and Ba, J. 2020. Maximum Entropy Gain Exploration for Long Horizon Multi-goal Reinforcement Learning. *arXiv preprint arXiv:2007.02832*.
- Pomerleau, D. A. 1989. Alvin: An autonomous land vehicle in a neural network. In *Advances in neural information processing systems*, 305–313.
- Raffin, A. 2018. RL Baselines Zoo. <https://github.com/araffin/rl-baselines-zoo>.
- Raffin, A.; Hill, A.; Ernestus, M.; Gleave, A.; Kanervisto, A.; and Dormann, N. 2019. Stable Baselines3. <https://github.com/DLR-RM/stable-baselines3>.
- Reynolds, D. A.; Quatieri, T. F.; and Dunn, R. B. 2000. Speaker verification using adapted Gaussian mixture models. *Digital signal processing* 10(1-3): 19–41.
- Ross, S.; Gordon, G.; and Bagnell, D. 2011. A reduction of imitation learning and structured prediction to no-regret online learning. In *Proceedings of the fourteenth international conference on artificial intelligence and statistics*, 627–635.
- Schulman, J.; Levine, S.; Abbeel, P.; Jordan, M. I.; and Moritz, P. 2015. Trust Region Policy Optimization. In *ICML*.
- Schulman, J.; Wolski, F.; Dhariwal, P.; Radford, A.; and Klimov, O. 2017. Proximal policy optimization algorithms. *arXiv:1707.06347*.
- Stanley, K. O.; and Miikkulainen, R. 2002. Evolving neural networks through augmenting topologies. *Evolutionary computation* 10(2): 99–127.
- Such, F. P.; Madhavan, V.; Conti, E.; Lehman, J.; Stanley, K. O.; and Clune, J. 2017. Deep neuroevolution: Genetic algorithms are a competitive alternative for training deep neural networks for reinforcement learning. *arXiv preprint arXiv:1712.06567*.
- Sutton, R. S.; and Barto, A. G. 2018. *Reinforcement learning: An introduction*. MIT press.
- Wang, Z.; Merel, J. S.; Reed, S. E.; de Freitas, N.; Wayne, G.; and Heess, N. 2017. Robust imitation of diverse behaviors. In *Advances in Neural Information Processing Systems*, 5320–5329.

## Appendix

### Environments and hyperparameters

#### Libraries

For the environments we use ones implemented in OpenAI Gym (Brockman et al. 2016). Experiments with RL algorithms use implementations from stable-baselines and stable-baselines3 libraries (for imitation learning) (Hill et al. 2018; Raffin et al. 2019), and evolutionary algorithms use NEAT and CMA-ES used in (Gaier and Ha 2019b), where CMA-ES is based on the PyCMA package (Hansen, Aki-moto, and Baudis 2019). For RL training hyperparameters we use parameters from rl-zoo (Raffin 2018). Behavioural cloning experiments use implementation from the “imitation” library<sup>1</sup>. For GMM and t-SNE implementations we use scikit-learn (Pedregosa et al. 2011). While not the most efficient, we opted for time-tested implementations to avoid errors in results because of fragile underlying algorithms.

#### Environments

Exact versions of the environments used are Acrobot-v0 (6D), Pendulum-v0 (3D), CartPole-v1 (4D), LunarLander-v2 (8D) and BipedalWalker-v3 (24D) from the OpenAI Gym library with their default settings. The dimensionality refers to the observation vector dimensionality, which is also used as a state for the policy supervector extraction. We selected these environments to cover tasks of different difficulty and state dimensionality, as latter influences the choice of different amounts of data.

For reward scaling (minimal and maximal reward), we use an approximate reward of a random agent for minimum and “reward threshold” for the maximum obtainable reward. Latter is defined by OpenAI Gym as reward that is required to solve the environment<sup>2</sup>. The minimum and maximum values are presented in Table 2.

#### Agent training hyperparameters

Agent training hyperparameters are provided in Table 3. RL hyperparameters use ones provided in rl-zoo (Raffin 2018) (without observation normalization), which improve the agent over time and in most cases train to optimal reward. For NEAT/CMA-ES hyperparameters we use ones used by Gaier and Ha (2019b) with exception of using 1024 generations for LunarLander and BipedalWalker, and 256 generations for the rest. Other parameters were set to the original for BipedalWalker and for the other environments we copy settings of SwingUp task. We limited the number of generations to reduce the amount of policies generated, which is enough in most environments to find a good solution (see Figure 6).

All RL agents use a neural network of two, 64-unit layers with tanh-activations for value and policy estimation (separate network for both), and policy actions are sampled from

the distribution parametrized by the final layer (discrete distribution). CMA-ES agents use fixed two-layer networks with sigmoid activations, with 40 units each for BipedalWalker and 5 units for other tasks. CMA-ES training terminates when fitness does not improve, which results in smaller cloud of points for CMA-ES in t-SNE figures.

#### Shared experimental setup and hardware

All experiments were ran on either four-core Intel Xeon W-2125, 64GB RAM workstation or on a 16-core Intel Xeon E5-2620 v4 (dual socket), 64GB RAM server machine. The only hard requirement for our experiments is the amount of system memory (64GB or more) and mass storage for storing policy trajectories (Approx. 300GB in total), and with above systems all of the experiments can be conducted in three to five days. Due to memory limitations we limited the data used to train the GMM-UBMs to 10M, which was randomly sampled from the set of all data. All experiments use diagonal covariance matrices (non-diagonal elements are zeros), which limits the expressive power of the GMM but provides much faster training speed, and which is commonly used in the speech processing. Data is standard-normalized  $((x - \mu)/\sigma)$  before training the GMM, and mean and standard deviation are stored along with the GMM for later use (policy supervectors).

All GMM-adaptation computations use relevance factor of  $r = 16$  and 64 Gaussian components for UBMs unless otherwise stated. Only one GMM is fitted per data, *i.e.* no multiple initialization and selecting the best fit. All repetitions are done with random seeds.

#### Experimental setup of component/amount of data experiments

We train three PPO agents on the environments and store 100 checkpoints of the policy during training (a set of policies), and then collect 200 trajectories of data per policy. We then sweep over the different amount of components (64, 32, 16, 8, 4, 2, 1) and number of trajectories per policy (100, 50, 25, 10), and for each combination train a GMM-UBM. The policy’s data is sampled from the originally gathered 200 trajectories. This process is repeated three times to simulate starting the method from a fixed set of policies (gathering data and training the GMM-UBM). In total we have nine different UBMs per environment per hyperparameters, each with their own corresponding set of policies (whose data was used to train the UBM).

**Distance between different policies.** For each policy we measure the average episodic reward over the 200 trajectories. If difference between rewards of two policies more than 25% of the total reward interval of the environment (see Table 2), these policies are treated as different. For each set of policies we then collect distances between all policies and distances between different policies, and compute the ratio between the averages of the two. These ratios are then averaged over the nine repetitions, which we report in the plots.

**Variance in distances.** For each set of policies we compute the distance between them and compute coefficient of variation over the three repetitions, where the sample stan-

<sup>1</sup><https://github.com/HumanCompatibleAI/imitation>

<sup>2</sup><https://github.com/openai/gym/wiki/Table-of-environments>

dard deviation is divided by the sample mean. Since underlying policies are the same (policies that generated the data), this value should approach zero. The result shown is then averaged over the three agents.

**Error in distances.** For each set of policies we compute distances between them all, and then one of the runs with 100 trajectories of data per policy is used as the anchor point / ground truth (one anchor for each different amount of components used). Then we measure relative error of distances obtained in other runs ( $|d - d_{\text{anchor}}|/d_{\text{anchor}}$ ), including the two other runs with 100 trajectories of data. Relative errors are first averaged over repetitions and then over agents.

### Experimental setup of evolution overview

We train five PPO agents and five A2C agents, storing 500 different versions of the policies during training. We also train a single run of NEAT and CMA-ES, and store 25% of the population candidates every tenth generation for further analysis. We then collect 100 trajectories of data per policy train one UBM per environment using data from all the policies. Due to memory constraints, we only used data from 100 randomly sampled policies per a single training run, after which we sample the 10M states to train the UBM. With UBMs we extract the policy supervectors and then run them all through a t-SNE using the KL-upper bound distance metric (Equation (6) in main paper).

### Experimental setup of PPO clip-ratio analysis

We train five PPO agents per different clip-ratio level (Table 4), where all other hyperparameters for training are the same except we set clip-ratio (and value function clip-ratio, as in original baselines implementation) to the studied value. We also train five A2C agents with the original settings for comparison. We store 50 policies over training, gather 100 trajectories per policy, train UBMs, extract policy-supervectors and compute distance between successive policies experienced during training (a vector of 49 values per one training run). We then sum these distances together for “total distance traveled”, average over the five repetitions and report the result. Pearson correlation is computed between current policy reward and distance to next policy, and averaged over repetitions and environments in the main paper.

### Experimental setup of imitation learning experiments

We train five PPO expert agents (from stable-baselines3 (Raffin et al. 2019)) on BipedalWalkerHardcore-v3 and LunarLander-v2, collect 10 trajectories of data and use it to train a behavioural cloning (BC) agent with 50 epochs over the data. After each epoch we store the current version of the BC policy. After training we collect additional 100 trajectories for the expert agent and for each BC policy, train the UBM, extract policy-supervectors and measure distance of all BC policies to the expert agent.

Environment	Min reward	Max reward
Pendulum-v0	-1600	-200
Acrobot-v1	-500	-100
LunarLander-v2	-230	200
BipedalWalker-v3	-100	300
CartPole-v1	0	500

Table 2: Min/Max values used for reward scaling per environment.

<b>PPO parameters</b>	<b>Bipedal.H.</b>	<b>Bipedal.</b>	<b>LunarLander</b>	<b>Acrobot</b>	<b>CartPole</b>	<b>Pendulum</b>
Environment steps trained	100 000 000	5 000 000	1 000 000	1 000 000	100 000	2 000 000
Number of environments	16	16	16	16	8	8
Rollout size	2048	2048	1024	256	32	2048
Training epochs	10	10	4	4	20	10
Batch size	1024	1024	512	512	256	512
Entropy loss weight	0.001	0.001	0.01	0.0	0.0	0.0
Policy ratio clip	0.2 (lin)	0.2	0.2	0.2	0.2 (lin)	0.2
Value ratio clip	0.2 (lin)	0.2	0.2	0.2	0.2 (lin)	0.2
Adam learning rate	0.00025 (lin)	0.00025	0.00025	0.00025	0.001 (lin)	0.0003
GAE $\lambda$	0.95	0.95	0.98	0.94	0.8	0.95
Discount factor	0.99	0.99	0.999	0.99	0.98	0.99
<b>A2C parameters</b>						
Environment steps trained	-	5 000 000	200 000	500 000	500 000	2 000 000
Number of environments	-	16	8	16	8	8
N-steps	-	5	5	5	5	5
Entropy loss weight	-	0.0	0.00001	0.0	0.0	0.0
RMSprop learning rate	-	0.0007 (lin)	0.00083 (lin)	0.0007	0.0007	0.0007
Discount factor	-	0.99	0.995	0.99	0.99	0.95
<b>NEAT parameters</b>						
Number of generations	-	1024	1024	256	256	256
Population size	-	192	128	128	128	128
<b>CMA-ES parameters</b>						
Number of generations	-	1024	1024	256	256	256
Population size	-	192	128	128	128	128

Table 3: Agent training hyperparameters. “(lin.)” marks parameters that are linearly decayed to zero over training. ”Bipedal.H.“ refers to BipedalWalkerHardcore, used in the imitation learning experiments with PPO expert agent.

$\epsilon$	Distance traveled					Corr( $R, d$ )				
	Bipedal	Lunar	Acro	Cart	Pend.	Bipedal	Lunar	Acro	Cart	Pend.
.01	23.6±1.1	4.5±.5	1.0±.1	2.0±.1	2.8±.4	.25±.18	-.06±.12	.46±.11	-.54±.07	-.13±.20
.1	1.7±1.5	9.9±.5	2.2±.1	7.7±1.6	1.2±.1	-.47±.19	-.25±.03	-.34±.23	-.14±.11	-.53±.04
.2	11.3±2.0	9.7±1.1	2.6±.2	13.6±1.0	1.3±.2	-.73±.08	-.34±.05	-.53±.21	-.01±.10	-.56±.11
.3	12.3±4.5	1.8±.4	2.5±.3	12.2±2.0	1.6±.3	-.61±.07	-.45±.11	-.43±.14	-.20±.14	-.33±.10
.4	11.9±2.3	14.7±2.3	2.4±.3	14.9±1.2	2.1±.5	-.66±.07	-.50±.05	-.40±.10	-.10±.09	-.42±.11
.5	12.0±2.6	15.0±.7	2.6±.1	15.3±1.7	2.5±.4	-.58±.12	-.43±.10	-.35±.13	.06±.24	-.19±.17
.75	17.7±7.4	16.7±1.0	2.5±.3	15.9±3.7	3.7±.5	-.54±.11	-.32±.09	-.40±.23	-.14±.28	.08±.09
1	25.1±1.9	18.9±2.5	2.6±.2	14.0±4.0	4.1±.6	-.60±.20	-.27±.06	-.37±.12	.23±.30	.11±.10
2	19.0±3.4	17.3±1.2	2.7±.2	17.1±4.6	3.5±.8	-.67±.10	-.15±.10	-.45±.22	-.15±.23	.04±.28
5	25.4±7.2	22.9±4.3	2.9±.3	2.2±2.6	3.4±.3	-.63±.14	.03±.13	-.47±.19	-.28±.17	.19±.18
10	51.5±21.1	21.5±2.6	2.8±.2	14.9±4.9	4.5±.7	-.58±.13	.03±.14	-.37±.18	.04±.39	.20±.26
A2C	61.8±16.6	29.4±4.3	2.2±.2	6.5±.7	9.8±2.4	-.46±.25	.40±.10	.20±.08	-.30±.12	.20±.18

Table 4: Full results of distance experiments with different PPO ratio-clip values, separated for each environment and averaged over five repetitions (including standard deviation over the five experiments).

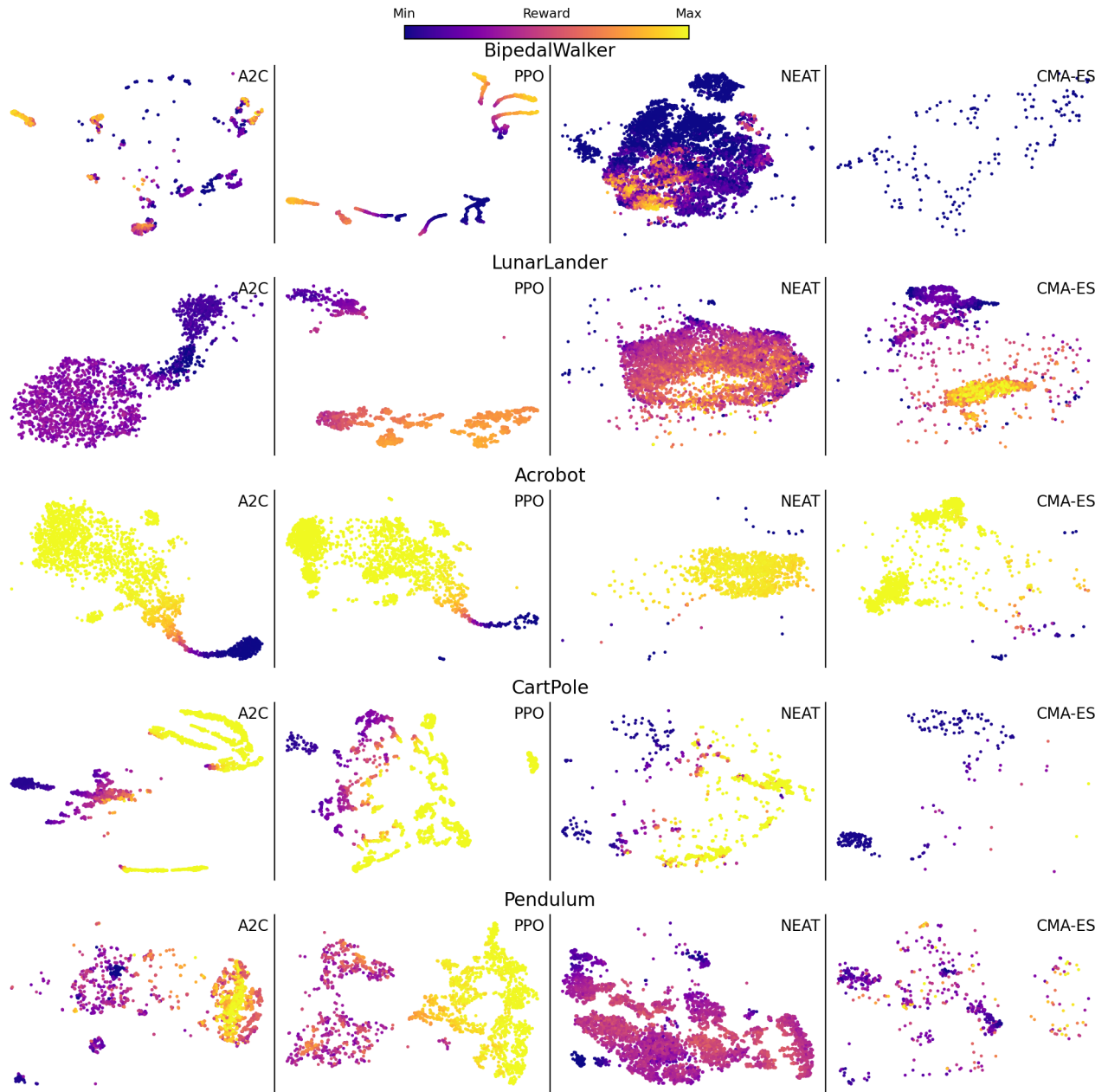


Figure 6: t-SNE plots of policies under different training algorithms in different environments.

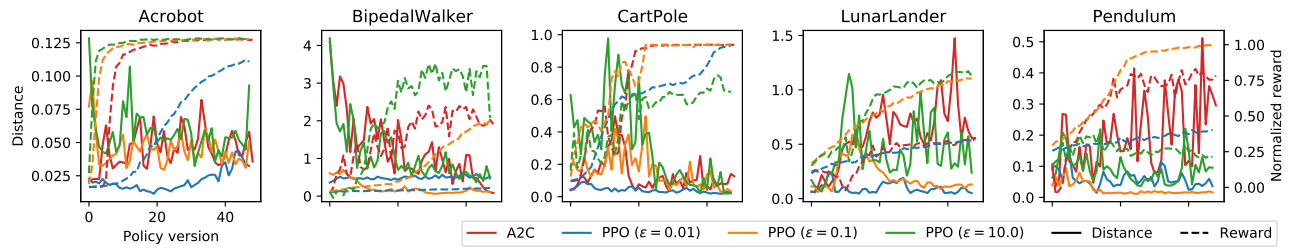


Figure 7: Learning curves with different clip-ratios  $\epsilon$  when using PPO, with A2C included for a comparison. Reward (dashed line) is normalized from minimum achievable reward (zero) to maximum (one). Distance refers to distance between successive policy versions. Curves are averaged over five repetitions. Variance is omitted for visual clarity.

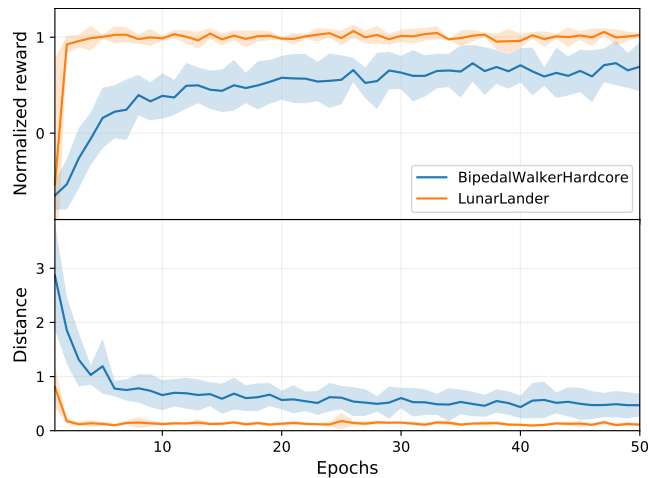


Figure 8: Behavioural cloning learning curves. Reward is normalized by dividing with expert's reward, with one equaling to performance of the expert. Distance refers to distance to the expert policy. Averaged over five repetitions. Shaded area represents plus-minus one standard deviation.

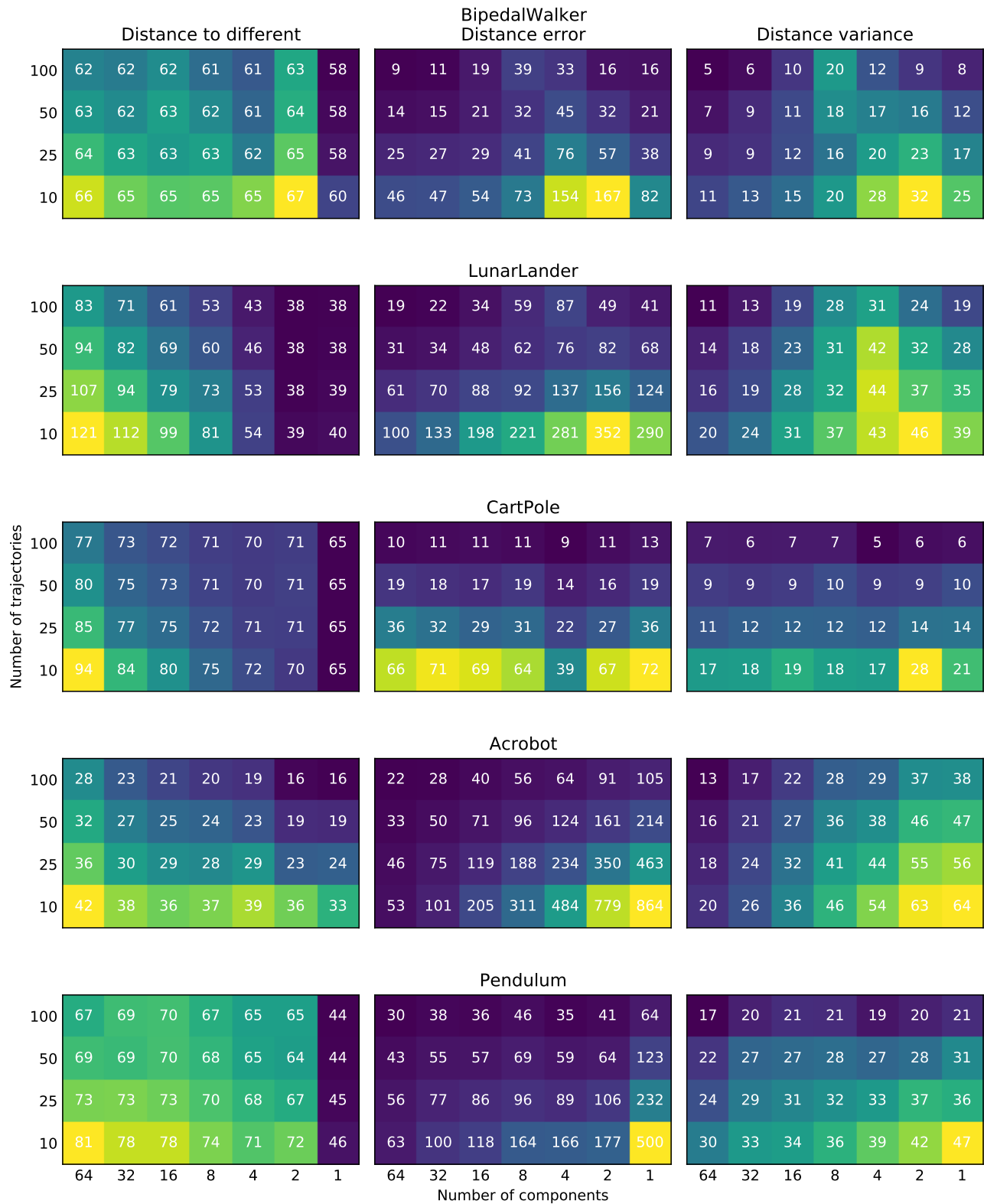


Figure 9: Lower is better. Per-environment results when analyzing the quality of final results under different amount of data per policy and GMM components. All values have been multiplied by hundred. Results have been averaged over three repetitions.